Towards enhancement of gas–liquid mass transfer in bioelectrochemical systems: Validation of a robust CFD model

eppendorf

The Smarter Solution

Flexible, powerful, industrial

Many engineering parameters need to be considered to establish a successful mAbs process. The BioFlo® 320 offers a wide range of options to meet your needs. It combines industrial design, flexibility between interchangeable autoclavable and single-use bioreactors, and universal gas control strategy for your applications.

> **New Scale Up Assist** software: Fast and easy calculation of important process parameter based on P/V or constant tip speed
> Compatible with the BioBLU® Single-use Bioreactor portfolio
> **Scalable:** Extensive working volume range of 250 mL – 40 L
> **Efficient:** Multi-unit control of up to eight systems from a single interface

www.eppendorf.com/BioFlo320

Received: 13 February 2021 | Revised: 22 May 2021 | Accepted: 7 June 2021

DOI: 10.1002/bit.27871

ARTICLE

BIOTECHNOLOGY AND BIOENGINEERING WILEY

Towards enhancement of gas–liquid mass transfer in bioelectrochemical systems: Validation of a robust CFD model

Mohsen Karimi[1] | Tove Widén[2] | Yvonne Nygård[2] | Lisbeth Olsson[2] | Henrik Ström[1]

[1]Department of Mechanical and Maritime Sciences, Division of Fluid Dynamics, Chalmers University of Technology, Gothenburg, Sweden

[2]Department of Biology and Biological Engineering, Division of Industrial Biotechnology, Chalmers University of Technology, Gothenburg, Sweden

Correspondence
Lisbeth Olsson, Department of Biology and Biological Engineering, Division of Industrial Biotechnology, Chalmers University of Technology, SE-41296 Gothenburg, Sweden.
Email: lisbeth.olsson@chalmers.se

Funding information
Swedish National Infrastructure for Computing; Chalmers Area of Advance Energy

Abstract

Mass transfer has been identified as a major bottleneck in gas fermentation and microbial conversion of carbon dioxide to chemicals. We present a pragmatic and validated Computational Fluid Dynamics (CFD) model for mass transfer in bioelectrochemical systems. Experiments were conducted to measure mixing times and mass transfer in a Duran bottle and an H-cell. An Eulerian–Eulerian framework with a simplified model for the bubble size distribution (BSD) was developed that utilized only one additional equation for the bubble number density while including the breakup and coalescence. Validations of the CFD model for mixing times showed that the predictions were within the confidence intervals of the measurements, verifying the model's capability in simulating the hydrodynamics. Further validations were performed using constant and varying bubble diameters for the mass transfer. The results showed the benefits of a simplified BSD model, as it yielded improvements of seven and four times in accuracy when assessed against the experimental data for the Duran bottle and H-cell, respectively. Modeling of the H-cell predicted that a lower stirring rate improves mass transfer compared with higher stirring rates, which is of great importance when designing microbial cultivation processes. The model offers a feasible framework for advanced modeling of gas fermentation and microbial electrosynthesis.

KEYWORDS
bubble number density, computational fluid dynamics, H-cells, mass transfer, microbial cultivations

1 | INTRODUCTION

The relevance of efficient mass transfer emerges in chemical, biochemical, and mineral processing industries where the primary response (e.g., separation, conversion, or dissolution) is susceptible to mass transfer intensification. Yet, the details of mass transfer on micro and macro scales have remained an active research topic for decades (Danckwerts, 1951; Higbie, 1935; Kawase et al., 1992; Lamont & Scott, 1970). The transfer of molecules from a gas phase to a liquid medium in gas–liquid systems is often a rate-limiting step

(Dhanasekharan et al., 2005; Rojas et al., 2021). To solve this problem, agitation is induced, which increases the interfacial area by generating many small gas bubbles. Mass transfer is directly proportional to the available gas surface area. Through agitation, mass transfer is thus enhanced at the cost of having to add kinetic energy to agitate the system. Agitation of the reactor is a very sensitive process parameter to control, as stirring is known to cause shear stress for the microorganisms, as reviewed by Böhm et al. (2019), and agitation of a bioreactor is a major cost for a biotechnological production process.

From an experimental perspective, the transfer rate of molecules from the gas phase to the liquid phase is measured via probing the molecules' dynamic concentrations as a function of time, which is typically presented as an overall mass transfer coefficient (i.e., $k_l \times a$) (e.g., Alves et al., 2004; Liu et al., 2019; Quijano et al., 2010; Schaepe et al., 2013). For instance, Labík et al. (2017) offered an expression, based on 1000 measurements of $k_l \times a$, that linked the overall mass transfer coefficient to impeller speed, superficial gas velocity, and power number.

A common format for these correlations is shown in Equation (1), where the forced convection via the *Re* number and the rate of diffusion of momentum over mass, that is, the *Sc* number, are related to the Sherwood number, *Sh*. The *Sh*, in turn, characterizes the ratio of convective to diffusive transport of the mass. The fitting constants are C, X, and Y, whereas l is a characteristic length scale (e.g., the bubble diameter) and D is the mass diffusivity.

$$Sh = \frac{k_l \times l}{D} = C \times (Re)^X (Sc)^Y. \quad (1)$$

The existence of a large number of empirical correlations attests to the fact that the current understanding of mass transfer in bubbly flows is still limited at the macroscopic level (Bach et al., 2017; Cussler, 2009; Garcia-Ochoa & Gomez, 2009; Rzehak & Krepper, 2016). For this reason, endeavors to accomplish mass transfer intensification in gas–liquid systems typically entail trial-and-error experimentations (Ansari et al., 2018; Zheng et al., 2018). Various innovative reactor systems (e.g., involving microbubbles, membranes, gas–liquid contactors, gas-diffusion electrodes, inventive fluid flow patterns and/or impeller designs) have been proposed (Bajracharya et al., 2016; Blanchet et al., 2015; Daniell et al., 2012; Köpke et al., 2011; Srikanth et al., 2018). Irrespective of the specific technological solution employed, the fundamental gas–liquid mass transfer process is the same, although the topology of the gas–liquid interface and the dynamics of the surrounding flow and concentration fields will differ on a case-by-case basis. It is not straightforward to carry over empirical expressions for the mass transfer rate from one reactor geometry to another. The underlying reason is that dissolved gas concentrations, mixing times, liquid turbulence, gas injection rates, and bubble sizes typically cannot be uniformly matched across different scales and geometries (Thomas et al., 2021; Yang, 2011). To complicate matters further, the application of novel concepts, such as microbial electrosynthesis methods, requires considerable changes to the reactor internals and therefore dramatically affect the fluid dynamics, consequently impacting the gas–liquid mass transfer (Bajracharya et al., 2016; Blanchet et al., 2015; Rosa et al., 2019). There is thus a need to assess the robustness of the gas–liquid mass transfer characterizations to the changes of reactor geometry and internals.

The evolution of modeling techniques has led the attention to hydrodynamic properties of bioreactors, and how they affect mass transfer (Godbole et al., 1984; Jones, 2007). A well-known drawback of empirical models is, however, the averaging process. In that, variables reflecting the hydrodynamic properties of the bioreactor (e.g., the velocity magnitude or the dissipation rate of turbulence) are averaged over the entire vessel generating uncertainties. A natural strategy to mitigate this problem is to shift the modeling toward a methodology in which the spatial and temporal variations of hydrodynamic properties are captured. Computational fluid dynamics (CFD) offers such an alternative to correlations and provides detailed information on the hydrodynamics of the flow. A drawback of current CFD methods is, however, the large computational cost associated with transient simulations in complex and large geometries.

For industrially relevant macro-scale CFD modeling, the Eulerian multifluid framework is most often used to simulate the continuous phase, the dispersed phase, and their interactions in bioreactors (Deen et al., 2002; Khopkar et al., 2005; Laakkonen et al., 2006). The level of details in modeling the dispersed phase could vary from the use of constant bubble diameter (Gakingo et al., 2020; Rzehak & Krepper, 2016), to a simplified bubble number density (BND) equation (Bakker, 1992; Lane et al., 2005), or to more complex population balance modeling (Amer et al., 2019; Gimbun et al., 2009; Kerdouss et al., 2008; Mishra et al., 2021; Ranganathan & Sivaraman, 2011; Scully et al., 2020). Single-phase modeling has also been used to investigate mixing time in high solids anaerobic digestion using different impeller types (Wu, 2012) or for optimization of sparger design in a pilot-scale photobioreactor when coupled with a first-order kinetic method (Ali et al., 2019). However, a major challenge in the development of robust CFD simulation methods for bubbly flows has been the tendency to validate these complicated models against experimental data sets with insufficient geometry variation, leaving important questions about applicability unanswered (Rzehak et al., 2015).

In the present work, our aim was to construct an experimentally validated, computationally viable, and robust CFD framework for mass transfer in bioelectrochemical systems. The model was developed to provide an understanding of the major resistance during the transfer of mass from the gas bubbles to the liquid from which the microbes can take up the gas. Such a model is a fundament for developing novel fermentation setups for utilizing microbes that has gas as the major energy and carbon source. The model integrates detailed hydrodynamic information to evaluate the mass transfer coefficient. In addition, it comprises significant physical phenomena occurring in the cultivations such as breakup and coalescence of gas bubbles. The model addresses the bubble size distribution (BSD) in a less expensive manner by solving only one additional scalar equation for the BND. This method in fact offers a pragmatic trade-off between accuracy and feasibility of the CFD model that also includes

the physical phenomena at the bubble scale such as breakup and coalescence using only one additional scalar equation. We developed and validated the method using two types of lab-scale cultivation vessels, a Duran bottle, and an H-cell. The vessels were both cylindrical and stirred by a magnetic stirrer. The gas was introduced as bubbles to the cultivation vessel via a diffusion stone. The two reactors differed in their internal volumes and in their smaller geometrical components, as well as in the presence and layout of reactor internals (e.g., electrode and probe). Experiments were carried out to validate mixing time and mass transfer coefficient. The focal point is to assess to what extent it is possible to establish an expression similar to Equation (1) that uses dimensionless numbers in describing the mass transfer and investigate whether such an equation can be robust to the changes in the reactor design. The current work lays a foundation for further investigations into the interactions of gas–liquid–microbe for bioelectrochemical systems using CFD and it aims to improve mass transfer of different gas (including syngas, consisting of CO, CO_2, and H_2) components to the microbes.

2 | MATERIALS AND METHODS

2.1 | Microbial cultivation setups

Two experimental setups were applied in the study; an H-cell reactor, which is commonly used for microbial conversion of carbon dioxide or other microbial electrosyntheses at lab scale, and a Duran bottle, used for anaerobic cultivations and providing a simplified version of the H-cell.

The H-cell reactor (Adams & Chittenden MFC 250.40.3, see Supporting Information for more details), schematically illustrated in Figure 1, consists of two identical chambers connected through a bridge but divided by a Nafion ion exchange membrane only allowing diffusion of ions between the different compartments. In a microbial electrosynthesis setup, one chamber contains the cathode, the microorganisms, and the substrate (carbon dioxide), while the other chamber contains the anode. Therefore, we studied mass transfer of a gas component added to the cathodic chamber. In the experiments, we used air to assess the changes in mass transfer instead of carbon dioxide with the assumption that the underlying mechanisms of the gas–liquid mass transfer for these gases are the same and that the transfer of both gases can thus be described by the same mathematical model (Köpke et al., 2011).

A 250 ml Duran bottle was used for initial testing and modeling. A cylindrical diffusion stone (10 mm in diameter, 20 mm high) connected to the gas inlet with tubing (8 mm in outer diameter) was placed 25 mm from the bottom of the bottle. A magnetic stirrer, approximately cylindrical with round edges (8 mm in diameter, 30 mm length), was placed at the bottom of the bottle, and an oxygen sensor (PreSens O_2 dipping probe PSt3, 5 mm in diameter, response time <6 s) was placed at the top of the bottle. The bottle was filled with 200 ml water. The cathodic chamber of the H-cell was filled with 270 ml water and a rectangular carbon felt cathode (25 × 70 mm); the cylindrical diffusion stone and the magnetic stirrer was placed as in the bottle, whereas the oxygen sensor was placed on the opposite side of the membrane with the tip 15 mm from the edge.

2.2 | Mixing time measurements

To assess how the mixing was affected by different stirring speeds and air flows, 100 µl of food coloring (Dr. Oetker) was added to the bottle and the mixing was filmed. The air flow was varied between

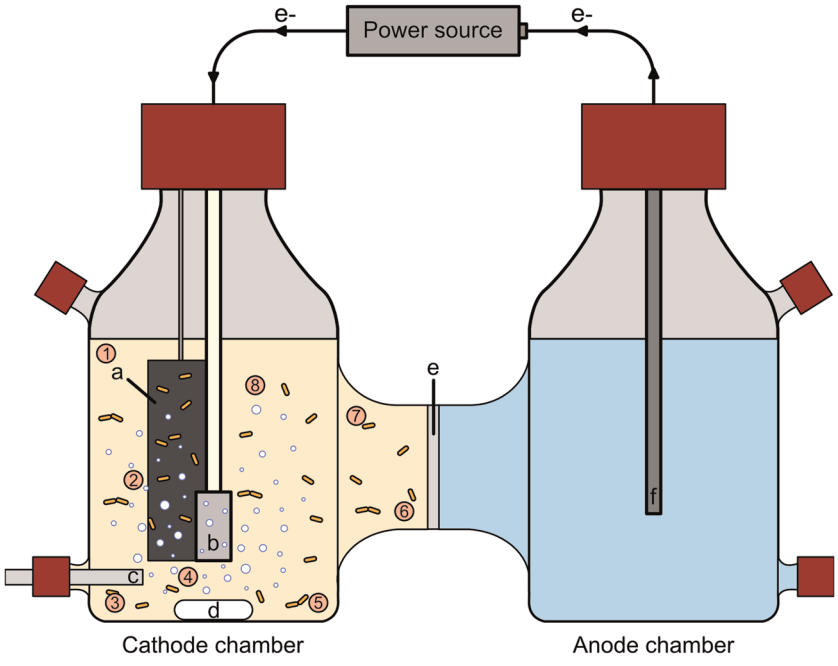

FIGURE 1 The H-cell reactor. (a) Carbon felt cathode; (b) sparger; (c) typically a reference electrode, in mass transfer experiments the oxygen sensor was placed here; (d) magnetic stirrer; (e) Nafion membrane; (f) anode [Color figure can be viewed at wileyonlinelibrary.com]

100, 200, and 400 ml/min, and the stirring between 100 and 300 rpm. Each condition was tested in triplicate. The videos were converted into image frames (10 images/s) using VLC Media Player and processed digitally using Fiji (Schindelin et al., 2012). The change in color intensity of eight reference points of the Duran bottle was determined over time. The reference points were selected so that their positions would reflect the different conditions in the bottle, being placed at different distances to the stirrer or the sparger (Figure 1). The mixing time was defined as the time from the injection of the dye until the coefficient of variation (in short, CoV) reached a value of 0.05, corresponding to 95% mixing or, equivalently, fluctuations around the final steady tracer concentration within ±5% (Bujalski et al., 2002).

2.3 | Mass transfer coefficient measurements

To obtain information about mass transfer, the change in dissolved oxygen was measured using the dynamic gassing-out method in the Duran bottle or H-cell setup as described in Section 2.1. The experiments were performed by sparging the bottle with N_2 through the diffusion stone until there was no dissolved oxygen detected and then switching to air until saturation. Stirring speeds of 100, 300, and 500 rpm, and air flows of 100, 200, and 400 ml/min were tested. The changes in oxygen concentration were measured throughout the experiment, and the value of $k_l \times a$ was obtained from the negative slope in the linear section of $\ln((C(t) - C^*)/(C(0)\text{-}C^*))$ versus t (Van't Riet, 1979).

3 | CFD MODEL

The Eulerian–Eulerian two-fluid model was employed to simulate gas bubbles and the continuous liquid phase inside the cultivation vessels. The continuity and momentum equations read as:

$$\frac{\partial(\alpha_i \rho_i)}{\partial t} + \nabla\cdot(\alpha_i \rho_i \mathbf{U}_i) = 0, \tag{2}$$

$$\frac{\partial(\alpha_i \rho_i \mathbf{U}_i)}{\partial t} + \nabla\cdot\left(\alpha_i \rho_i \mathbf{U}_i \mathbf{U}_i\right) = -\alpha_i \nabla p + \alpha_i \rho_i \mathbf{g} + \nabla\cdot\left(\alpha_i \tau_i - \alpha_i \rho_i \overline{\mathbf{u}_i' \mathbf{u}_i'}\right) + \vec{F}_d, \tag{3}$$

where for phase index i (continuous phase $i = 1$, and dispersed phase $i = 2$), α is the phase volume fraction, ρ is the phase density, and $\mathbf{U}$ is the velocity field. The time, pressure, gravitational acceleration, and drag force per unit volume are represented by t, p, $\mathbf{g}$, and $\vec{F}_d$. The viscous stress tensor is τ_i, while the Reynolds stresses due to fluctuating components of the velocities are represented by, $\overline{\mathbf{u}_i' \mathbf{u}_i'}$. The standard k–ε turbulence model was applied to determine the turbulent characteristics of the mixture phase and to compute the turbulent viscosity. The conservation equations for k and ε can be found in Ansys (2013).

Furthermore, the model should support the variation of bubble sizes in the cultivation vessels as the distribution of the dispersed phase translates into the available interfacial area, which, in turn, directly affects the modeling predictions of the mass transfer coefficients. Nevertheless, classical gas–liquid models assumed an average diameter for the entire computational domain (e.g., see Deen et al., 2002; Gosman et al., 1992). In this study, we have demonstrated how this assumption alters the $k_l \times a$ predictions.

Population balance equation (PBE) is the most general practice to estimate the BSD (Amer et al., 2019; Marchisio & Fox, 2013). The solution methods for PBE can be classified into two groups: (a) representing the BSD by different size classes, MUSIGs (Laakkonen et al., 2007), and (b) tracking moments of a distribution (Marchisio et al., 2003) (i.e., different tastes of quadrature approximations). Both methods, even though proven to be accurate, come with the extra computational load of solving several transport equations. A simpler yet somewhat less frequently used approach to deal with the size distribution of bubbles is to solve a single scalar equation for the BND accounting for coalescence and breakup (Bakker, 1992; Lane, 2006; Moilanen, 2009). The method has the potential to accelerate otherwise expensive CFD simulations. For instance, in predicting $k_l \times a$, Moilanen et al. (2008) reported that applying a BND approach halved the computational time compared with MUSIGs with insignificant differences in the results. Therefore, to lay down a computationally affordable model, we have also adopted the BND approach. The derivation of the governing equations was presented by Lane (2006) and is summarized in the Supporting Information.

As stated earlier, the quantity of interest for computing the mass transfer coefficient is the *Sh* number. From dimensional analysis, the *Sh* number is found to be a function of the *Re* number and the *Sc* number, characterizing the forced convection due to stirring and the relation between diffusion of momentum and mass, respectively. To study this concept, we exploited Equation (1), to compute the values of k_l by employing the local values of velocity, the bubble diameters, and the interfacial area ($a = 6\alpha_2/d_b$).

$$Sh = k_l \times \frac{d_b}{D} = C\,(Re)^X\,(Sc)^Y \Rightarrow k_l = \frac{D}{d_b} \times C\,(Re)^X\,(Sc)^Y. \tag{4}$$

Cussler (2009) stated that the model constants are case-dependent, for example, for packed towers, the dependency on the fluid velocity varies about 0.7 power while for the diffusion coefficient, it ranges between 0.5 and 0.7 power. In this study, the constants were determined by fitting to the simulation results at 300 rpm and 200 ml/min: $C = 1.2$, $X = 1/2$, and $Y = 1/3$.

We also seek to understand whether the accuracy and the additional cost of a simplified model for the BSD were justified. Thus, we also evaluated the predictions obtained by Equation (5), which is specifically derived for gas bubbles in stirred tanks (Cussler, 2009). This expression has similar dependencies on the hydrodynamics, bubble diameter, and *Sc* number as Equation (4).

$$Sh = 0.13\left(\frac{\left(\frac{P}{V}\right)d_b^4}{\rho_1 \nu^3}\right)^{0.25}\left(\frac{\nu}{D}\right)^{0.33}. \tag{5}$$

where P/V is the stirred power per volume.

4 | RESULTS AND DISCUSSION

We first validated the capability of the model to describe the mixing of a tracer in the Duran bottle. After that, we assessed the predictions of the mass transfer coefficient obtained for this reactor and investigated the sensitivity to the exact formulation used in Equation (1). Finally, we shifted to the H-cell to evaluate the robustness of the results obtained in the bottle for this cultivation vessel of similar shape but with different internals.

4.1 | Modeling mass transfer in a Duran bottle

Mixing time is a global parameter in cultivation vessels that indicates the hydrodynamics of the system, and we choose the mixing time as a first validation of the flow prediction obtained from the CFD model. The simulations were designed to mirror the experiments by patching a passive scalar at the injection point and monitoring the scalar values in different locations over the simulation time. Thirty probes were chosen to encompass different zones in the computational domain and to be able to capture the mixing dynamics. The CoV values for different operational conditions were evaluated according to 30, 14, and 5 probes and no significant variations were found.

Figure 2 shows a CoV curve quantifying the mixing characteristics in the bottle. To provide a better visual understanding, the snapshot images from the experiments were imposed on the plot at three time instances including injection time, 95% mixing time, and 99% mixing time. The choice of mixing criterion (i.e., CoV = 0.05) clearly corroborated with the visual uniformity of the dye from the experiments and thus it was capable of accurately predicting the mixing time. Given the findings presented in Figure 2, a set of mixing time simulations was carried out under different operational conditions to assess the model performance before simulations of mass transfer.

The numerical predictions of mixing time for different experiments, as well as statistical details of the measurements, are summarized in Table 1. The mixing experiments were carried out with and without the presence of air bubbles and with and without rotational effects. As expected, due to the increase in the level of turbulence at higher stirring rates (Experiments 1–3), less time was needed to reach homogeneity, a trend that was also captured by the CFD predictions. The largest error of 32% occurred for the lowest rotational speed, although the predicted value for this experiment

TABLE 1 Validation of mixing time prediction in the bottle under different operational conditions

Experiment	Stirring speed (rpm)	Airflow rate (ml/min)	Experiments Mean mixing time (s)	*SD*	CFD predictions (s)
1	300	0	3.1	0.80	2.1
2	500	0	1.9	0.14	1.8
3	800	0	1.2	0.27	1.4
4	0	200	5.6	2.83	3.8
5	0	400	4.8	0.71	3.5
6	300	200	3.3	0.57	2.4

Abbreviation: CFD, computational fluid dynamics.

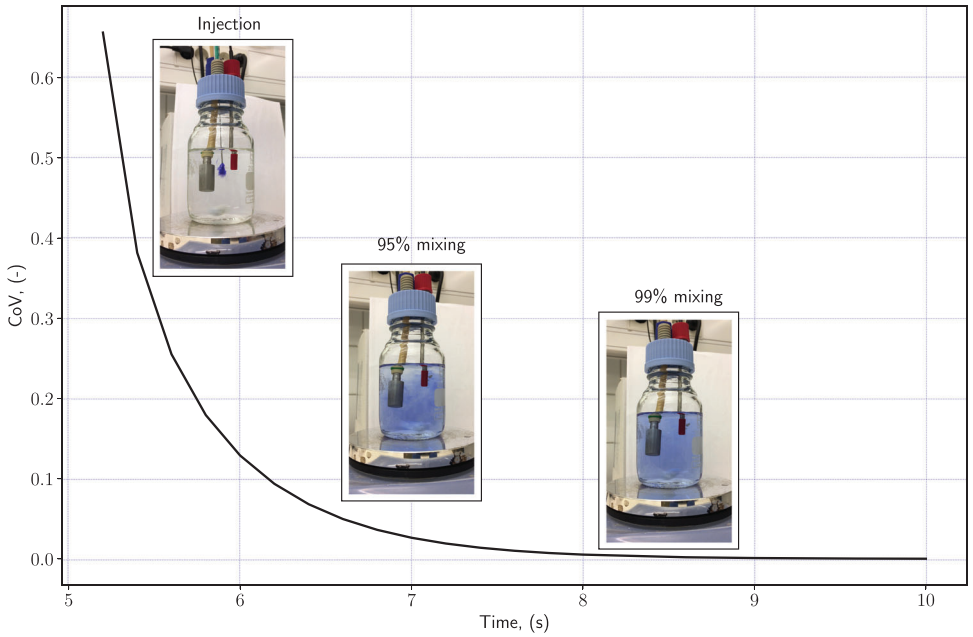

FIGURE 2 Coefficient of variation (CoV) plot for computing mixing time and corresponding snapshots of the experiments [Color figure can be viewed at wileyonlinelibrary.com]

still fell within the 95% confidence interval of the experiment. The smallest error for simulations without air was only 5% for the highest stirring speed. The main reason for the better agreement at higher stirring rates is most likely related to the higher turbulent intensity, for which the k–ε turbulence model should be better suited. The experiments with air bubbles showed that the effects of stirring were more dominant compared with the presence of gas bubbles while sparging the gas through the diffusion stone. An interesting observation appeared when comparing Experiments 1 and 6, where sparging air into the system somewhat prolonged the mixing time, an effect that was also captured by the CFD predictions. This implies that the contribution of bubble-induced turbulence in the mixing was insignificant at the current conditions and that the gas flow may to some extent counteract mixing between the aerated sections and the bulk of the liquid.

The idea behind the validation by mixing time was to utilize a practical approach for preliminary validation of the CFD model. The choice of CoV among other criteria for the evaluation of mixing time was also shown to be a credible method for the mixing time evaluation. Therefore, we concluded that the predictive capability of the CFD model for the flow hydrodynamics was established. The first level of validations by mixing time was then extended by predictions of mass transfer coefficients. Equation (4) was employed to obtain the local values of $k_l \times a$ using two different approaches including assumed constant bubble diameters and a BND implementation.

Measurements were performed under constant rotational speed and increasing airflow rates (Table 2). They showed that increasing the gas flow rate improved the mass transfer, which is explained by the presence of more air bubbles (i.e., an increased interfacial area). The numerical predictions also captured the increasing trend both when using constant bubble diameters and the BND implementation. A great improvement in the accuracy of the numerical predictions was observed when using the BND model for the BSD. For instance, at the low gas flow rate, the errors in predictions dropped approximately four- and sevenfold using Equations (4) and (5), respectively. Similar improvements were also attained for Experiment 2 in Table 2; the error in predictions of $k_l \times a$ decreased from 39% to 29% using Equation (4) and fivefold using Equation (5). To compare the two expressions, a constant bubble diameter of $d_b = 1\,\text{mm}$ was opted for. This choice of bubble diameter was motivated based on a formulation for the bubble diameter at a sparger in low gas flow rates proposed by Seader et al. (1997). Comparing the two expressions with constant bubble diameter, one can establish that the use of local *Re* numbers in Equation (4) for describing the hydrodynamics of the flow yields better predictive performance, as the model specifically derived for a stirred tank failed to predict the experiments at higher gas flow rates. On the contrary, integrating the BSD resulted in the same magnitudes of error for both expressions. It is worth noting that this level of accuracy was achieved by adding only one scalar equation to the CFD framework.

4.2 | Modeling mass transfer in an H-cell

Having validated the CFD-BND model for the bottle, evaluations of the model robustness were performed for the mass transfer coefficients in a different cultivation vessel, an H-cell. Table 3 summarizes the results from the measurements in the H-cell. In this vessel, the airflow rate has a more controlling effect on the mass transfer than the rotational speed of the capsule. For instance, comparing Experiments 1 (100 rpm, 200 ml/min) and 2 (300 rpm, 100 ml/min) in Table 3 reveals that even though the rotational speed was increased, the mass transfer coefficient was reduced by 49% due to less air in the system. This observation is a particularly important reminder of the significant challenges faced when trying to model mass transfer at similar conditions (e.g., bubbly air–water flow at similar airflow rates and stirring speeds) but in a reactor design slightly different from the one in which the mass transfer modeling was originally developed and validated.

Simulations were also conducted to test the CFD model using the experimental data in (Table 3). As for the bottle, a constant bubble diameter ($d_b = 1\,\text{mm}$) and the BND implementation were compared using Equations (4) and (5).

The effects of stirring on the $k_l \times a$ values under constant air flow rate for measurements and simulations are shown in Figure 3. The increasing trend of experiments for angular velocity >300 rpm was captured with both approaches (Equations 4 and 5). We, therefore, performed two more simulations for 650 and 800 rpm to establish how this trend continues. The reason

TABLE 3 Summary of $k_l \times a$ experimental measurements for H-cell under different operational conditions

Experiment	Stirring speed (rpm)	Airflow rate (ml/min)	Experiments	
			Mean $k_l \times a$ (1/s)	*SD*
1	100	200	0.005828	0.000918
2	300	100	0.002946	0.000749
3	300	200	0.004488	0.001671
4	500	200	0.005139	0.001106

TABLE 2 Experimental measurements and numerical validations of mass transfer coefficients for the Duran bottle

Experiment	Stirring speed (rpm)	Airflow rate (ml/min)	Experiments		Current work (Equation 4)		Stirred tank (Equation 5)	
			Mean $k_l \times a$ (1/s)	*SD*	d_b = 1 (mm)	BND	d_b = 1 (mm)	BND
1	300	200	0.003678	0.000711	0.002776	0.003920	0.001870	0.003395
2	300	400	0.004253	0.000454	0.005902	0.005471	0.009135	0.005288

Abbreviation: BND, bubble number density.

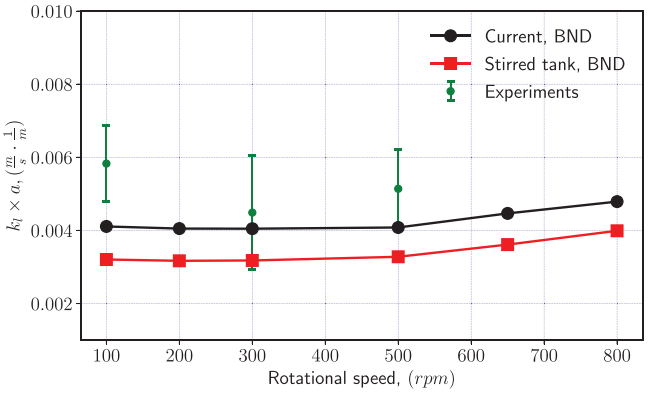

FIGURE 3 Experimental data and computational fluid dynamics predictions of mass transfer coefficients for constant gas flow rate [Color figure can be viewed at wileyonlinelibrary.com]

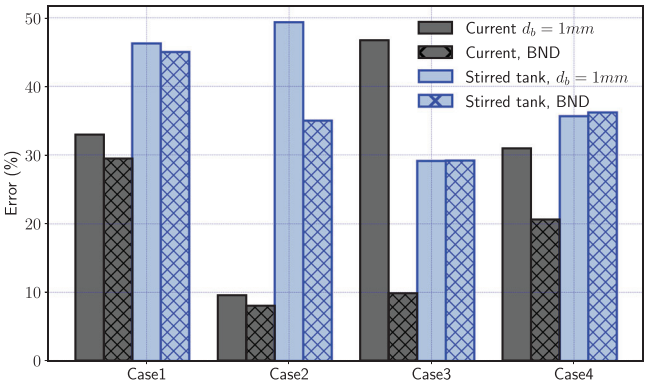

FIGURE 4 Error bars for the prediction of mass transfer coefficients in the H-cell. The filled bars are for bubble number density (BND) errors, the dark color is for the current study (Equation 4), and the light color for the stirred tank expression [Color figure can be viewed at wileyonlinelibrary.com]

for the increasing mass transfer coefficient is explained by the higher turbulence dissipation in the system, leading to the breakup of more bubbles and creating more available surface area. This phenomenon is echoed in the breakup source term (see Supporting Information) via having a greater number of cells with *We* number higher than We_{cr}, which leads to more breakups in the model. On the contrary, measurements showed that by decreasing the capsule speed from 300 to 100 rpm an increase in the mass transfer coefficient occurred. This observation is highly relevant for designing microbial cultivation experiments where a higher rotational speed is otherwise often favored. A lower stirring could further improve the process by creating less shear stress and provide cost savings. However, the two models predicted flat lines when decreasing the rotational velocity. This discrepancy could possibly be explained by the uncertain quality of the turbulence model predictions at the lowest stirring rates, in combination with not accounting for saturation effects in the liquid phase in the current simulations.

Figure 4 is a bar plot illustrating the errors in the predictions of mass transfer coefficients for the experiments reported in Table 3. It is immediately visible that Equation (4) with the BND performed better in all cases regardless of the operational conditions. The improvements for the four cases with the BND ranged from approximately 2% in Experiment 1 to fourfolds in Experiment 3 that distinctly confirmed the use of the BSD for H-cell simulations. The predictions with the expression for the stirred tank (Equation 5), on the contrary, showed improvements for the first two experiments, whereas no significant differences were observed for the other experiments. In comparison to the methods employed in this study for prediction of mass transfer coefficient in the bottle (Equation 4), the BND implementation performed better in all simulations (Table 3). The level of improvement was attributed to two components of the framework; first, the use of local *Re* to incorporate the hydrodynamics of the flow and second, including the bubble diameter variations instead of applying a constant value.

5 | CONCLUSIONS

The main aim in this study was to provide a new and more efficient modeling approach for bubbly flow mass transfer in cultivation vessels. The predicted values for the mixing times always fell within the confidence intervals of the experimental data, verifying that the hydrodynamics of the cultivation vessels were simulated successfully. Furthermore, the results confirmed the accuracy gained by the BND implementation for the BSD. In that, comparing the $k_l \times a$ predictions using constant and varying bubble diameters showed maximum improvements of seven- and fourfold for the bottle and H-cell, respectively. Simulating the mass transfer in the two types of vessels showed that a more general *Sh* correlation is preferable in terms of robustness when varying the hydrodynamics. Moreover, when applying the CFD framework to a different reactor geometry, the importance of local *Re* numbers and BND become more important. Remarkably, the modeling of the H-cell predicted that a lower stirring speed may improve mass transfer compared with a higher stirring speed. In summary, the results obtained from the two-step validations of the CFD model lay a foundation for future investigations into the mass transfer at the gas–liquid–microorganisms level.

ACKNOWLEDGMENTS

The simulations were performed on resources at the Chalmers Centre for Computational Science and Engineering (C3SE) provided by the Swedish National Infrastructure for Computing (SNIC). The research was funded by the Chalmers Area of Advanced Energy.

AUTHOR CONTRIBUTIONS

Lisbeth Olsson and Henrik Ström conceptualized the study. Mohsen Karimi and Henrik Ström designed and performed the modeling work. Tove Widén, Yvonne Nygård, and Lisbeth Olsson designed the experimental work and Tove Widén performed the experimental work. Mohsen Karimi drafted the major parts of the manuscript with

contributions from Henrik Ström and Tove Widén. All authors contributed to the analysis and interpretation of data and shaping of the manuscript. All authors read the final version and approved it.

DATA AVAILABILITY STATEMENT

The data that support the findings of this study are available from the corresponding author upon request.

ORCID

Lisbeth Olsson http://orcid.org/0000-0002-0827-5442
Henrik Ström http://orcid.org/0000-0002-8581-5174

REFERENCES

Ali, H., Solsvik, J., Wagner, J. L., Zhang, D., Hellgardt, K., & Park, C. W. (2019). CFD and kinetic-based modeling to optimize the sparger design of a large-scale photobioreactor for scaling up of biofuel production. *Biotechnology and Bioengineering*, *116*(9), 2200–2211. https://doi.org/10.1002/bit.27010

Alves, S. S., Maia, C. I., & Vasconcelos, J. M. T. (2004). Gas-liquid mass transfer coefficient in stirred tanks interpreted through bubble contamination kinetics. *Chemical Engineering and Processing: Process Intensification*, *43*(7), 823–830. https://doi.org/10.1016/S0255-2701(03)00100-4

Amer, M., Feng, Y., & Ramsey, J. D. (2019). Using CFD simulations and statistical analysis to correlate oxygen mass transfer coefficient to both geometrical parameters and operating conditions in a stirred-tank bioreactor. *Biotechnology Progress*, *35*, e2785. https://doi.org/10.1002/btpr.2785

Ansari, M., Turney, D. E., Yakobov, R., Kalaga, D., Kleinbart, S., Banerjee, S., & Joshi, J. B. (2018). Chemical hydrodynamics of a downward microbubble flow for intensification of gas-fed bioreactors. *American Institute of Chemical Engineers Journal*, *64*(4), 1399–1411. https://doi.org/10.1002/aic.16002

Ansys. (2013). *Ansys fluent theory guide* (Vol. 15317). ANSYS Inc.

Bach, C., Yang, J., Larsson, H., Stocks, S. M., Gernaey, K. V., Albaek, M. O., & Krühne, U. (2017). Evaluation of mixing and mass transfer in a stirred pilot scale bioreactor utilizing CFD. *Chemical Engineering Science*, *171*, 19–26. https://doi.org/10.1016/j.ces.2017.05.001

Bajracharya, S., Vanbroekhoven, K., Buisman, C. J. N., Pant, D., & Strik, D. P. B. T. B. (2016). Application of gas diffusion biocathode in microbial electrosynthesis from carbon dioxide. *Environmental Science and Pollution Research*, *23*, 22292–22308. https://doi.org/10.1007/s11356-016-7196-x

Bakker, A. (1992). *Hydrodynamics of stirred gas-liquid dispersions* (February 1992), 135. https://doi.org/10.13140/RG.2.2.11733.01767

Blanchet, E., Duquenne, F., Rafrai, Y., Etcheverry, L., Erable, B., & Bergel, A. (2015). Importance of the hydrogen route in up-scaling electrosynthesis for microbial CO_2 reduction. *Energy & Environmental Science*, *8*, 3731–3744. https://doi.org/10.1039/C5EE03088A

Böhm, L., Hohl, L., Bliatsiou, C., & Kraume, M. (2019). Multiphase stirred tank bioreactors—New geometrical concepts and scale-up approaches. *Chemie-Ingenieur-Technik*, *91*(12), 1724–1746. https://doi.org/10.1002/cite.201900165

Bujalski, J. M., Jaworski, Z., Bujalski, W., & Nienw, A. W. (2002). The influence of the addition position of a tracer on CFD simulated mixing times in a vessel agitated by a Rushton turbine. *Chemical Engineering Research and Design*, *80*, 824–831. https://doi.org/10.1205/026387602321143354

Cussler, E. L. (2009). *Diffusion mass transfer in fluid systems*. Cambridge University Press.

Danckwerts, P. V. (1951). Significance of liquid-film coefficients in gas absorption. *Industrial & Engineering Chemistry*, *43*(6), 1460–1467. https://doi.org/10.1021/ie50498a055

Daniell, J., Köpke, M., & Simpson, S. D. (2012). Commercial biomass syngas fermentation. *Energies*, *5*, 5372–5417. https://doi.org/10.3390/en5125372

Deen, N. G., Solberg, T., & Hjertager, B. H. (2002). Flow generated by an aerated Rushton impeller: Two-phase PIV experiments and numerical simulations. *Canadian Journal of Chemical Engineering*, *80*(4), 1–15. https://doi.org/10.1002/cjce.5450800406

Dhanasekharan, K. M., Sanyal, J., Jain, A., & Haidari, A. (2005). A generalized approach to model oxygen transfer in bioreactors using population balances and computational fluid dynamics. *Chemical Engineering Science*, *60*(1), 213–218. https://doi.org/10.1016/j.ces.2004.07.118

Gakingo, G. K., Clarke, K. G., & Louw, T. M. (2020). A numerical investigation of the hydrodynamics and mass transfer in a three-phase gas-liquid-liquid stirred tank reactor. *Biochemical Engineering Journal*, *157*, 107522. https://doi.org/10.1016/j.bej.2020.107522

Garcia-Ochoa, F., & Gomez, E. (2009). Bioreactor scale-up and oxygen transfer rate in microbial processes: An overview. *Biotechnology Advances*, *27*(2), 153–176. https://doi.org/10.1016/j.biotechadv.2008.10.006

Gimbun, J., Rielly, C. D., & Nagy, Z. K. (2009). Modelling of mass transfer in gas-liquid stirred tanks agitated by Rushton turbine and CD-6 impeller: A scale-up study. *Chemical Engineering Research and Design*, *87*(4), 437–451. https://doi.org/10.1016/j.cherd.2008.12.017

Godbole, S. P., Joseph, S., Shah, Y. T., & Carr, N. L. (1984). Hydrodynamics and mass transfer in a bubble column with an organic liquid. *American Institute of Chemical Engineers Journal*, *30*(2), 213–220. https://doi.org/10.1002/cjce.5450620326

Gosman, A. D., Lekakou, C., Politis, S., Issa, R. I., & Looney, M. K. (1992). Multidimensional modeling of turbulent two-phase flows in stirred vessels. *American Institute of Chemical Engineers Journal*, *38*(12), 1946–1956. https://doi.org/10.1002/aic.690381210

Higbie, R. (1935). The rate of absorption of a pure gas into a still liquid during short periods of exposure. *Transactions of the Institution of Chemical Engineers*, *31*, 365–389.

Jones, S. T. (2007). *Gas liquid mass transfer in an external airlift loop reactor for syngas fermentation*. Iowa State University.

Kawase, Y., Halard, B., & Moo-Young, M. (1992). Liquid-phase mass transfer coefficients in bioreactors. *Biotechnology and Bioengineering*, *39*(11), 1133–1140. https://doi.org/10.1002/bit.260391109

Kerdouss, F., Bannari, A., Proulx, P., Bannari, R., Skrga, M., & Labrecque, Y. (2008). Two-phase mass transfer coefficient prediction in stirred vessel with a CFD model. *Computers and Chemical Engineering*, *32*(8), 1943–1955. https://doi.org/10.1016/j.compchemeng.2007.10.010

Khopkar, A. R., Rammohan, A. R., Ranade, V. V., & Dudukovic, M. P. (2005). Gas-liquid flow generated by a Rushton turbine in stirred vessel: CARPT/CT measurements and CFD simulations. *Chemical Engineering Science*, *60*, 2215–2229. https://doi.org/10.1016/j.ces.2004.11.044

Köpke, M., Mihalcea, C., Bromley, J. C., & Simpson, S. D. (2011). Fermentative production of ethanol from carbon monoxide. *Current Opinion in Biotechnology*, *22*, 320–325. https://doi.org/10.1016/j.copbio.2011.01.005

Laakkonen, M., Alopaeus, V., & Aittamaa, J. (2006). Validation of bubble breakage, coalescence and mass transfer models for gas-liquid dispersion in agitated vessel. *Chemical Engineering Science*, *61*(1), 218–228. https://doi.org/10.1016/j.ces.2004.11.066

Laakkonen, M., Moilanen, P., Alopaeus, V., & Aittamaa, J. (2007). Modelling local gas–liquid mass transfer in agitated vessels. *Chemical Engineering Research and Design*, *85*, 665–675. https://doi.org/10.1205/cherd06171

Labík, L., Moucha, T., Petříček, R., Rejl, J. F., Valenz, L., & Haidl, J. (2017). Volumetric mass transfer coefficient in viscous liquid in mechanically agitated fermenters. Measurement and correlation. *Chemical Engineering Science*, *170*, 451–463. https://doi.org/10.1016/j.ces.2017.04.006

Lamont, J. C., & Scott, D. S. (1970). An eddy cell model of mass transfer into the surface of a turbulent liquid. *American Institute of Chemical Engineers Journal*, *16*(4), 513–519. https://doi.org/10.1002/aic.690160403

Lane, G. L. (2006). *Computational modelling of gas-liquid flow in stirred tanks*. The University of Newcastle.

Lane, G. L., Schwarz, M. P., & Evans, G. M. (2005). Numerical modelling of gas-liquid flow in stirred tanks. *Chemical Engineering Science*, *60*, 2203–2214. https://doi.org/10.1016/j.ces.2004.11.046

Liu, K., Phillips, J. R., Sun, X., Mohammad, S., Huhnke, R. L., & Atiyeh, H. K. (2019). Investigation and modeling of gas-liquid mass transfer in a sparged and non-sparged continuous stirred tank reactor with potential application in syngas fermentation. *Fermentation*, *5*(3):75. https://doi.org/10.3390/fermentation5030075

Marchisio, D. L., & Fox, R. (2013). *Computational models for polydisperse particulate and multiphase systems*. Cambridge University Press.

Marchisio, D. L., Vigil, R. D., & Fox, R. O. (2003). Quadrature method of moments for aggregation-breakage processes. *Journal of Colloid and Interface Science*, *258*(2), 322–334. https://doi.org/10.1016/S0021-9797(02)00054-1

Mishra, S., Kumar, V., Sarkar, J., & Rathore, A. S. (2021). CFD based mass transfer modeling of a single use bioreactor for production of monoclonal antibody biotherapeutics. *Chemical Engineering Journal*, *412*, 128592. https://doi.org/10.1016/j.cej.2021.128592

Moilanen, P. (2009). *Modelling gas-liquid flow and local mass transfer in stirred tanks*. Helsinki University of Technology.

Moilanen, P., Laakkonen, M., Visuri, O., Alopaeus, V., & Aittamaa, J. (2008). Modelling mass transfer in an aerated 0.2 m^3 vessel agitated by Rushton, Phasejet and Combijet impellers. *Chemical Engineering Journal*, *142*, 95–108. https://doi.org/10.1016/j.cej.2008.01.033

Quijano, G., Chávez-Avila, R., Muñoz, R., Thalasso, F., & Ordaz, A. (2010). k_La measurement in two-phase partitioning bioreactors: New insights on potential errors at low power input. *Journal of Chemical Technology and Biotechnology*, *85*(10), 1407–1412. https://doi.org/10.1002/jctb.2460

Ranganathan, P., & Sivaraman, S. (2011). Investigations on hydrodynamics and mass transfer in gas-liquid stirred reactor using computational fluid dynamics. *Chemical Engineering Science*, *66*(14), 3108–3124. https://doi.org/10.1016/j.ces.2011.03.007

Rojas, M. del P. A., Zaiat, M., Gonzalez, E. R., De Wever, H., & Pant, D. (2021). Enhancing the gas–liquid mass transfer during microbial electrosynthesis by the variation of CO_2 flow rate. *Process Biochemistry*, *101*, 50–58. https://doi.org/10.1016/j.procbio.2020.11.005

Rosa, L. F. M., Hunger, S., Zschernitz, T., Strehlitz, B., & Harnisch, F. (2019). Integrating electrochemistry into bioreactors: Effect of the upgrade kit on mass transfer, mixing time and sterilizability. *Frontiers in Energy Research*, *7*, 1–11. https://doi.org/10.3389/fenrg.2019.00098

Rzehak, R., & Krepper, E. (2016). Euler-Euler simulation of mass-transfer in bubbly flows. *Chemical Engineering Science*, *155*, 459–468. https://doi.org/10.1016/j.ces.2016.08.036

Rzehak, R., Krepper, E., Liao, Y., Ziegenhein, T., Kriebitzsch, S., & Lucas, D. (2015). Baseline model for the simulation of bubbly flows. *Chemical Engineering & Technology*, *38*, 1972–1978. https://doi.org/10.1002/ceat.201500118

Schaepe, S., Kuprijanov, A., Sieblist, C., Jenzsch, M., Simutis, R., & Lübbert, A. (2013). k_La of stirred tank bioreactors revisited. *Journal of Biotechnology*, *168*(4), 576–583. https://doi.org/10.1016/j.jbiotec.2013.08.032

Schindelin, J., Arganda-Carreras, I., Frise, E., Kaynig, V., Longair, M., Pietzsch, T., Preibisch, S., Rueden, C., Saalfeld, S., Schmid, B., Tinevez, J. Y., White, D. J., Hartenstein, V., Eliceiri, K., Tomancak, P., & Cardona, A. (2012). Fiji: An open-source platform for biological-image analysis. *Nature Methods*, *9*(7), 676–82.

Scully, J., Considine, L. B., Smith, M. T., McAlea, E., Jones, N., O'Connell, E., Madsen, E., Power, M., Mellors, P., Crowley, J., O'Leary, N., Carver, S., & Van Plew, D. (2020). Beyond heuristics: CFD-based novel multiparameter scale-up for geometrically disparate bioreactors demonstrated at industrial 2kL–10kL scales. *Biotechnology and Bioengineering*, *117*(6), 1710–1723. https://doi.org/10.1002/bit.27323

Seader, J. D., Siirola, J. J., & Barnicki, S. D. (1997). *Perry's chemical engineer's handbook*. McGraw-Hill.

Srikanth, S., Singh, D., Vanbroekhoven, K., Pant, D., Kumar, M., Puri, S. K., & Ramakumar, S. S. V. (2018). Electro-biocatalytic conversion of carbon dioxide to alcohols using gas diffusion electrode. *Bioresource Technology*, *265*, 45–51. https://doi.org/10.1016/j.biortech.2018.02.058

Thomas, J. A., Liu, X., DeVincentis, B., Hua, H., Yao, G., Borys, M. C., Aron, K., & Pendse, G. (2021). A mechanistic approach for predicting mass transfer in bioreactors. *Chemical Engineering Science*, *237*, 116538. https://doi.org/10.1016/j.ces.2021.116538

Van't Riet, K. (1979). Review of measuring methods and results in nonviscous gas-liquid mass transfer in stirred vessels. *Industrial & Engineering Chemistry, Process Design and Development*, *18*, 357–364. https://doi.org/10.1021/i260071a001

Wu, B. (2012). CFD simulation of mixing for high-solids anaerobic digestion. *Biotechnology and Bioengineering*, *109*(8), 2116–2126. https://doi.org/10.1002/bit.24482

Yang, S.-T. (Ed.). (2011). *Bioprocessing for value-added products from renewable resources: New technologies and applications*. Elsevier. https://doi.org/10.1016/B978-0-444-52114-9.X5000-2

Zheng, Z., Chen, Y., Zhan, X., Gao, M., & Wang, Z. (2018). Mass transfer intensification in a novel airlift reactor assembly with helical sieve plates. *Chemical Engineering Journal*, *342*, 61–70. https://doi.org/10.1016/j.cej.2018.01.039

SUPPORTING INFORMATION

Additional Supporting Information may be found online in the supporting information tab for this article.

How to cite this article: Karimi, M., Widén, T., Nygård, Y., Olsson, L., & Ström, H. (2021). Towards enhancement of gas–liquid mass transfer in bioelectrochemical systems: Validation of a robust CFD model. *Biotechnology and Bioengineering*, 1–9. https://doi.org/10.1002/bit.27871